Hund's coupling and its key role in tuning multiorbital correlations

Luca de' Medici

Laboratoire de Physique des Solides, UMR8502 CNRS-Universite Paris-Sud, Orsay, France

It is shown how, in multiband materials, the Hund's coupling plays a crucial role in tuning the degree of electronic correlation. While in half-filled systems it enhances the correlations, in all other cases it pushes the boundary for the Mott transition at very high critical couplings. Moreover in weakly hybridized nondegenerate systems the Hund's coupling plays the role of band decoupler, causing a change from a collective to an individual band behavior, due to the freezing of orbital fluctuations. In this situation the physics is strongly dependent on individual filling and electronic structure of each band, and orbital-selective Mott transitions (or even a cascade of such transitions) are to be expected. More generally a heavy differentiation in the actual degree of correlation of different bands arises and the system can show both weakly and strongly correlated electrons.

PACS number(s): 71.30.+h, 71.27.+a, 71.10.Fd

I. INTRODUCTION

Correlated materials are a continuous source of new and intriguing phenomena in condensed matter physics. The realizable stoichiometric structures of compounds partially filling $3d$, $4d$, $5d$, $4f$, or $5f$ orbitals are virtually endless, and many of the explored ones have shown an extremely rich physics as a function of external parameters such as pressure, temperature, magnetic field, and chemical substitutions.

This rich and varied physics is in many cases a direct outcome of electron-electron interactions and of the subtlety of the many-body physics that they yield.

The "correlation strength" is the relevance of these many-body effects for the conduction electrons. These effects are indeed related to the interaction coupling strength in the conduction bands (but not always simply proportional to, as we will see in this paper), compared with their width (or more precisely the kinetic energy of the bare conduction electrons). The coupling strength is maximal in the mentioned orbitals in that they have a reduced spatial extension, which maximizes the Coulomb interaction within the shell, yet they are filled after the bigger s and p shells of higher principal quantum number, thanks to the aufbau "inversion" rule. Thus, e.g., the $4s$ are filled before the $3d$ orbitals and determine the atomic positions such that the overlap of the $3d$ orbitals and the corresponding bandwidth are rather small.

However these correlated orbitals are degenerate (five-fold for the d and seven-fold for the f) in isolated atoms, and different behaviors arise in real solids depending on whether the crystal field due to the surrounding atoms lifts this degeneracy.

In materials where the degeneracy is totally lifted, only one band crosses the Fermi level and is thus partially filled, and a one-orbital tight-binding model is often enough for a description of the low-energy physics. In this case the ratio between the interorbital interaction strength U and the bandwidth W is the control parameter of the many-body effects.

When several correlated orbitals contribute to the conduction bands instead, more parameters come into play, and a richer many-body phenomenology is to be expected. Besides the more complicated band structure, the number of parameters needed to describe the electron-electron interaction is increased. Interorbital interactions are different from intraorbital

ones, and Hund's rule, the tendency of electrons to distribute in different orbitals and in high-spin states, plays a role.

In a multiband tight-binding low-energy model the Hamiltonian reads in general

$$H = \sum_{ij,mm'\sigma} t_{ij}^{mm'} d_{im\sigma}^{\dagger} d_{jm'\sigma} + H_{\text{int}}, \qquad (1)$$

where $d_{im\sigma}^{\dagger}$ creates an electron with spin σ in orbital m on the site i and $t_{ij}^{mm'}$ are the hopping amplitudes. The local interaction vertex can be written as

$$\begin{aligned}
H_{\text{int}} = &\ U \sum_{i,m} n_{im\uparrow} n_{im\downarrow} + \left(U' - \frac{J}{2}\right) \sum_{i,m>m'} n_{im} n_{im'} \\
&- J \sum_{i,m>m'} [2\mathbf{S}_{im} \cdot \mathbf{S}_{im'} + (d_{im\uparrow}^{\dagger} d_{im\downarrow}^{\dagger} d_{im'\uparrow} d_{im'\downarrow} + h.c.)],
\end{aligned} \qquad (2)$$

where $n_{im\sigma} = d_{im\sigma}^{\dagger} d_{im\sigma}$, $n_{im} = \sum_\sigma n_{im\sigma}$, and $\mathbf{S}_{im} = \frac{1}{2} \sum_{\sigma\sigma'} d_{im\sigma}^{\dagger} \boldsymbol{\tau}_{\sigma\sigma'} d_{im\sigma'}$, where $\boldsymbol{\tau}_{\sigma\sigma'}$ is the Pauli matrices vector. U is the intraorbital interaction, U' is the interorbital one ($U' = U - 2J$ holds from symmetry reasons on the matrix elements[1,2]), and J is the Hund's exchange coupling. J can be seen then as a measure of the dependence of the interaction strength on the electrons occupying the same or different orbitals, and on their mutual spin alignment.

Among many tools for the investigation of correlated materials through the analysis of these low-energy models, slave-variable mean fields (the most well known being the slave bosons, SBs)[3,4] and dynamical mean field theory (DMFT)[5] have achieved much success. These are nonperturbative local mean fields and have been successful in describing many aspects of correlated systems as band renormalization and mass enhancement, magnetic orders, and the Mott transition.

The latter is the the transition between a paramagnetic metal and a paramagnetic insulator because of the localization of conduction electrons due to interactions. It is relevant to many materials[6] and it has also been invoked to explain the physics of high-temperature superconductors.[7] The physics in the proximity of the Mott transition has some well-defined features that deserve the christening with a specific name: "Mottness." These include strong quasiparticle mass renormalization and

sizable spectral weight transfer from low-energy coherent to high-energy incoherent features, among others.

The metallic phase in proximity to a Mott transition is a paradigm of strongly correlated physics, and its analysis has been performed in detail in the one-band Hubbard model.[5]

At present there is less understanding of the Mott physics and in general of the effect of interactions in multiband models. Early studies[8,9] have clarified that the Mott transition is found at any integer filling and in N-band degenerate systems with bandwidth W and $SU(2N)$ symmetric interaction, i.e., $J = 0$, the critical interaction strength U_c/W grows with the degeneracy N and is maximal at half-filling.

The dependence of the Mott transition critical coupling U_c/W as a function of Hund's coupling J was studied in Refs. [10]–[12]. In all these studies J is shown to *reduce* the U_c/W needed for the Mott transition, and thus to correlate the electrons. However, these studies are restricted to half-filled systems, and the generality of this statement for the Mott transitions at all integer fillings is questionable.

Recently, the role of Hund's coupling has been brought under the spotlight by the discovery of iron-based superconductors[13,14] in which this coupling within the Fe orbitals is believed to be sizable. Metallic iron is known to have a strong Hund's coupling, leading to ferromagnetism, and this is expected to be true also in the Fe atoms of these compounds. Moreover local density approximation + DMFT calculations have shown extreme sensitivity of some aspects of the physics of Fe superconductors to the Hund's coupling strength.[15]–[18] In these materials six electrons occupy five correlated bands, all crossing the Fermi level, mainly of Fe character. The application to this case of the present knowledge of Hund's coupling effect is not obvious.

One of the main results of this paper (Sec. III) is that for all integer fillings of a degenerate Hubbard model, beside global half-filling, the Hund's coupling actually *increases* the critical U needed for the Mott transition, bringing it to very large values for reasonable coupling strength, contrary to the previously studied half-filled cases.

Many other aspects of the physics of Fe superconductors are still subject to a debate in the scientific community, and many competing scenarios have been put forward, without reaching consensus thus far. The possibility of these materials being in or in proximity to an orbital-selective Mott phase in which some localized electrons coexist with itinerant ones has been invoked by several groups.[19]–[22] The mechanism possibly leading to an orbital-selective Mott transition[23] (OSMT) in these materials was first isolated in Ref. [24] and shown to be related to the strong Hund's coupling.

The other main result (Sec. IV) of this paper is the highlighting of Hund's coupling as the main factor responsible in general for the arising of the OSMT in real nondegenerate (for the presence of a crystal field splitting or different band dispersions) weakly hybridized systems. Overriding or accompanying bandwidth differences and degeneracies, Hund's coupling is seen to act as a *band decoupler*, through the suppression of orbital fluctuations. Then the correlation character of each band is determined by its individual filling and structure. This mechanism also applies to the well-known anomalous superconductor Sr_2RuO_4, as has been recently outlined in Ref. [25].

II. MODELS AND TECHNIQUES

We will solve model Eq. (1) with slave-spin mean field (SSMF)[26,27] and DMFT.[5]

SSMF is a computationally fast slave-variable mean field particularly suited for studying multiband models. It is extremely useful for tracing entire phase diagrams and yields qualitatively accurate and semiquantitative results, in line with the performance of usual SBs. But unlike the latter, which become quickly untractable in the multiband case, SSMFs limit the proliferation of auxiliary variables and can thus tackle, e.g., a five-band model and trace a phase diagram as a function of several parameters. As all other slave-variable methods do, at the mean field level SSMF approximates the model with a quasiparticle effective noninteracting model whose parameters are self-consistently determined. Solving a local problem for the slave variable takes into account the effect of interactions and yields the quasiparticle effective parameters, i.e., renormalization of the crystal field and of the electron mass. The latter is expressed through the quasiparticle renormalization factor Z_m, which ranges from 1 (noninteracting system) to 0 and whose vanishing signals a Mott transition.

For supporting the SSMF results, and reporting aimed and quantitatively accurate results, we make use of the well-established DMFT which is also heavier to run. DMFT assumes the locality of the self-energy and maps the (multiorbital) lattice problem onto a (multiorbital) quantum impurity problem subject to a self-consistency condition. The impurity problem has to be solved numerically, and we use the Lanczos exact diagonalization[28] as the impurity solver. Details about these two mean-field methods are given in the appendix.

In all cases we consider nonhybridized bands, i.e., $t_{ij}^{mm'} = t_{ij}^m \delta_{mm'}$. We then discuss how our analysis is affected by a finite (small) hybridization.

The two methods being local mean fields, in absence of hybridization the k dependence enters the problem only through each band dispersion. Sums over momenta can thus be replaced by integrals over energy weighted by density of states (DOS) $D(\epsilon)$, which we assume to be semicircular throughout the paper, i.e.,

$$D(\epsilon) = \frac{2}{\pi D} \sqrt{1 - (\epsilon/D)^2}, \tag{3}$$

where $D = W/2$ is the half-bandwidth.

Then a model is fully specified by each band's width and position, the latter being set by the crystal field splitting, i.e., by the set of on-site energy levels $\epsilon_m \equiv t_{ii}^m$.

We solve the model in different cases: N-fold degenerate model in Sec. III, the three-band model with same bandwith and trigonal crystal field splitting, and with three different bandwidths but without the crystal field in Sec. IV.

We will assume zero temperature throughout the paper.

III. HUND'S COUPLING AND THE MOTT TRANSITION IN DEGENERATE SYSTEMS

We first study the N-fold degenerate Hubbard model at all possible integer fillings. All N bands have $D = 1$ and no crystal field splitting is present, i.e., $\epsilon_m = 0$.
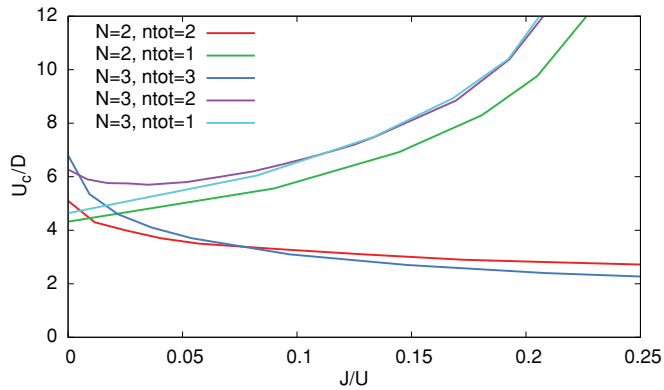
FIG. 1. (Color online) SSMF metal-Mott insulator critical coupling U_c for the N-band degenerate Hubbard model as a function of the ratio J/U. Only fillings such that $n < N$ are shown here. The ones for $n > N$ give identical results due to particle-hole symmetry. For half-filled cases (two electrons in two bands and three electrons in three bands) the Hund's coupling correlates the system and reduces the critical U_c/D. For all other fillings, on the contrary, U_c/D is strongly increased.

Figure 1 shows the results of the SSMF. At all integer filling n we find, as known, that for increasing U at fixed J/U the renormalization factor Z_m—identical for all bands—decreases from unity, reaching zero beyond a critical U_c/D and thus signaling a Mott transition. At $J = 0$ our analysis confirms that U_c is maximum for half-filling and that for a given filling n/N, U_c increases with the degeneracy N (see Ref. 8).

We then study the dependence of U_c/D on the value of J. At half-filling ($n = 2$ electrons in $N = 2$ bands, or $n = 3$ electrons in $N = 3$ bands in Fig. 1) we find that increasing J/U reduces the value of U_c, as reported in previous works.[10–12,29]

But surprisingly, for any other filling U_c *is rather increased by Hund's coupling*.

We see this in detail for the two-band case in Fig. 2. On going from $J = 0$ to a typical value $J/U = 0.25$, the critical interaction strength is reduced to half of its original value at half-filling, but it increases to more than three times the $J = 0$ value for the quarter-filled case.

This result is general and does not depend on the number of bands. In the three-band model the reduction of U_c at half-filling is even stronger than in the two-band case, while the behavior of the system with one electron follows the trend of the analogous case in the two-band system. Interestingly a slightly different behavior can be noticed in the case of two electrons in three bands. Here the onset of J induces initially a reduction of U_c, which quickly starts increasing again and follows the trend of the other non-half-filled cases, with the Mott transition pushed at very strong couplings.

Hints of this physics can be seen in Ref. 30 where the opposite trend of the different ($n = 1, 2, 3$) Mott insulating lobes of the phase diagram as a function of J was reported. To understand these opposite trends we will follow an argument based on the analysis of the atomic limit.[10,30,31]

Indeed an estimate of U_c can be obtained following Mott's original image for the single-band case: At strong coupling the local spectral function of a Mott insulator shows features based on the atomic excitations (two delta functions at a distance U
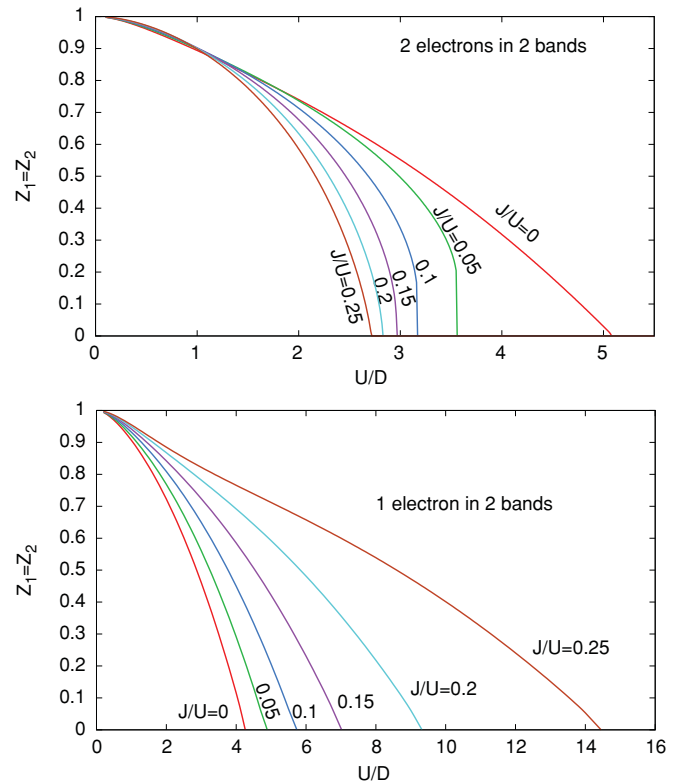

FIG. 2. (Color online) Quasiparticle renormalization factor Z for the two-band Hubbard model as function of the interaction strength U and for different values Hund's coupling J. Upper panel: half-filled case. Lower panel: quarter-filled case. The effect of the Hund's coupling is opposite in the two cases.

from one another), broadened by the delocalization energy which can in principle be calculated perturbatively in t/U. In practice these broadened features (called the "Hubbard bands") have a width in energy of the order of the bare bandwidth W. Thus an estimate of the Mott gap is the distance of the borders of these two features, i.e., $\Delta = U - W$. By the same token an estimate of the critical U for the Mott transition is given by the vanishing of the gap, i.e., $U_c/W = 1$, which is not far from the $U_{c1}/W \simeq 1.2$ obtained by full-fledged DMFT.

The full many-body physics is more complicated,[32] and in these estimates one should for example take into account the dependence of the delocalization energy, and thus of the width of the Hubbard bands, on the physical parameters. In practice, at least in the Hubbard model, this is seen to be a minor effect and only very close to the transition does one see sizable deviations from $\Delta = U - W$.

Transposing this argument to the multiorbital case we thus want to obtain the scaling with Hund's J of the Mott gap and of the U_c for the Mott transition in the multiband Hubbard model. In Fig. 3 is depicted the atomic excitation spectrum for a 2-orbital atom. A change in the atomic spectrum will reflect directly on the distance between the Hubbard bands and then on the Mott gap. The 16 states are divided in sectors with the same number of particles, whose distance is set by U. Instead within every sector, for a given particle number, the states are split by J.
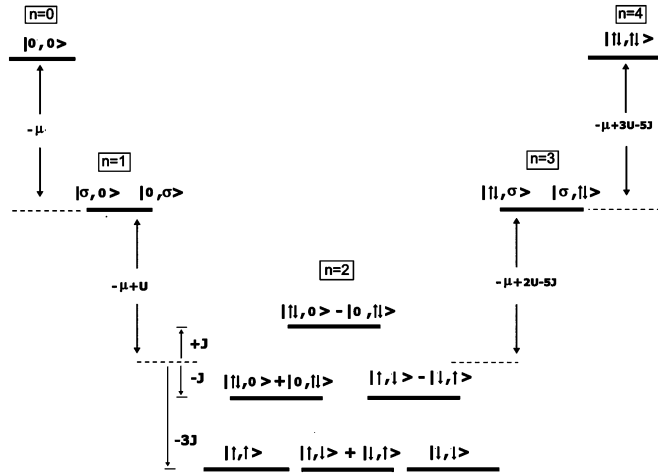
FIG. 3. Spectrum of a 2-orbital atom with Hamiltonian Eq. (2). The different sectors position in energy is as depicted for an half-filled system, for which the chemical potential can be obtained by particle-hole symmetry arguments and is $\mu = (3U - 5J)/2$ and the ground state lies in the $n = 2$ sector. In general the distance of this with the lowest lying state in the $n = 3$ sector is $E_0^3 - E_0^2 = -\mu + 2U - 2J$ whereas the distance with the lowest lying state in the $n = 1$ sector is $E_0^1 - E_0^2 = \mu - U + 3J$. The atomic gap is then $\Delta = U + J$ and thus is enhanced by J.

The global filling of the system is set by the chemical potential which shifts the relative position of the different sectors. When the system is half-filled μ is such that the ground state is in the 2-particle sector. For any finite J this is 3-fold degenerate and is the triplet of $S = 1$ states. The gap in the atomic excitation spectrum is obtained summing the energy distance between the ground state and the lowest lying levels (E_0) in the $n + 1$ and $n - 1$ sectors, i.e.,

$$\Delta^{at} = E_0^{n+1} - E_0^n + E_0^{n-1} - E_0^n = E_0^{n+1} + E_0^{n-1} - 2E_0^n. \tag{4}$$

This quantity is readily evaluated, yielding

$$\Delta^{at} = U + J. \tag{5}$$

It is independent of μ and shows that the gap is enlarged by J. In the Mott insulator then, if we assume that the Hubbard bands are broadened versions of the atomic excitations the gap will also scale linearly in J, and so will U_c/D (with opposite sign, because a larger gap will close, when the Hubbard bands overlap, at a smaller U).

Let's now replicate this argument for the quarter-filled case. In the corresponding atomic spectrum (Fig. 4) the lowest lying sector is the one with $n = 1$. The atomic gap is now

$$\Delta^{at} = U - 3J, \tag{6}$$

which is reduced by J. Thus the U_c for the Mott insulator with 1 particle (or 3) in 2 bands will get enhanced by J.

The same argument applies in general for any number N of bands, to show that the Mott gap gets reduced in all cases but at half-filling. It is easy to calculate that in general

$$\Delta_n^{at} = \begin{cases} U - 3J, & \forall n \neq N \quad \text{(off half-filling)}, \\ U + (N-1)J, & n = N \quad \text{(half-filling)}. \end{cases} \tag{7}$$
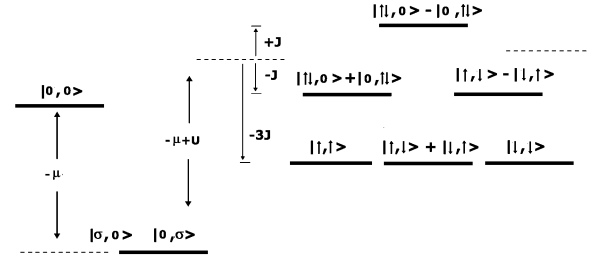

FIG. 4. Same as in Fig. 3 but the sector's position in energy is depicted here for the system quarter-filled. The distance with the $n = 2$ sector is $E_0^2 - E_0^1 = -\mu + U - 3J$ whereas the distance with the $n = 0$ sector is $E_0^0 - E_0^1 = \mu$. The atomic gap is then $\Delta = U - 3J$ and is then reduced by J.

The rationale behind this is as follows. The energy of the high-spin state in each sector is lowered by the exchange among the electrons which is proportional to the number of possible pairs of aligned spare spins. The latter is maximum in the half-filled sector where there is one spare electron in every orbital. Moving away from half-filling, it decreases quadratically, because the number of the possible pairs is $n_s(n_s - 1)/2$, where n_s is the number of spare electrons, which decreases while the number of either empty or fully occupied orbitals increases.

Thus the gap in a half-filled Mott insulator is always enhanced by J, being enhanced by the distance between the ground state and the lowest state in the neighboring sectors.

In the case of a Mott insulator with a non-half-filled ground state (say without loss of generality lying in the sector with $n < N$ particles) this has a gain in energy due to J which is smaller than the one for the high-spin state of the neighboring sector (with $n + 1$ particles) closer to (or at) half-filling and bigger than the one with $n - 1$ particles due to the mentioned quadratic dependence. The latter is also responsible for the fact that the subsequent enhancement of $E_{n-1} - E_n$ with J is less than the reduction of $E_{n+1} - E_n$. The overall gap is then reduced.

The same obviously applies for the particle-hole symmetric situation for $n > N$.

The estimate of the dependence of U_c on J, following these arguments, is

$$\delta U_c(n) \propto \begin{cases} 3J, & \forall n \neq N \quad \text{(off half-filling)}. \\ -(N-1)J, & n = N \quad \text{(half-filling)} \end{cases} \tag{8}$$

Figure 5 plots the SSMF phase diagram as a function of J, and we compare the results with these asintotic behaviors based on the atomic limit, Eq. (8). It is clear that at strong J the atomic limit captures perfectly the dependence of U_c.

However, departures from these analytic results are found at weak J. The previous argument basis indeed, is that J is large enough for only the high-spin state to be taken into account in each sector. This assumption is not justified at weak J, and orbital fluctuations become important when taking into account the hopping from site to site. These are maximal at $J = 0$, and the consequent gain in kinetic energy is the cause for the enhancement of U_c with the band degeneracy.[33] The onset of J suppresses these fluctuations rapidly and we thus observe a quick reduction of U_c in the half-filled systems, where the orbital fluctuations are maximal. Moving away from
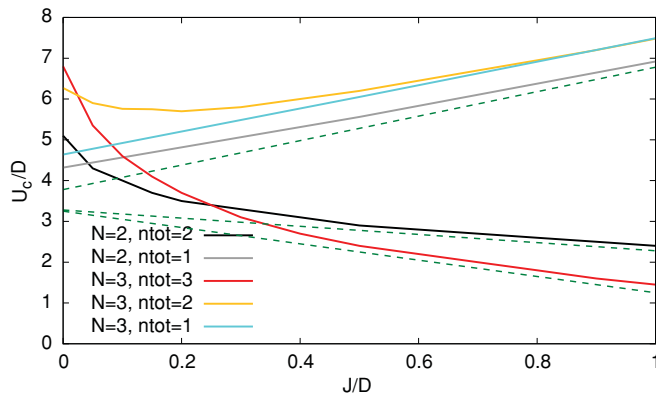
FIG. 5. (Color online) Same phase diagram as in Fig. 1, plotted here as a function of J. The dashed lines indicate the strong J behavior calculated analytically in the atomic limit, Eq. (8) (from top to bottom $\delta U_c \propto 3J, -J, -2J$).

half-filling this effect is controlled by n/N (for $n < N$, and by the particle-hole symmetric $(N - n)/N$ for $n > N$), and it is already negligible for the system with one particle in three bands. The reduction of orbital correlations is in fact a main effect of J, and we will see in Sec. IV its key importance in decoupling the orbitals.

It is worth stressing that these conclusions are drawn for degenerate nonhybridized bands but are still valid for small hybridizations $V_{mm'}$ and crystal fields $\Delta_{mm'} = \epsilon_m - \epsilon_{m'}$. Indeed both hybridization and crystal fields work in general "against" J (the hybridization favors singlet states, while the crystal field favors orbital disproportionation, both thus favor low-spin states[29]), but are nonsingular perturbations.

Thus if $J \gg V_{mm'}, \Delta_{mm'}$ we expect these results to hold in general.

More specifically one can show that their effect on the high-spin states in the atomic limit is null in the half-filled sector and lowers the energy in sectors away from half-filling. The detail of this energy gain depends in general on the specific structure of the matrices $V_{mm'}, \Delta_{mm'}$, and its analysis is beyond the scope of this paper, but it can be easily shown for $N = 2$ and 3 that they always reduce the effect of J on the gap between the atomic sectors and will thus reduce the effect of J on U_c. Some specific models with finite crystal fields are studied in Sec. IV.

SSMF and atomic limit considerations are somewhat complementary points of view on the Mott transition and they draw a quite reliable picture, but one may want to benchmark these results with a more quantitative and accurate method such as DMFT.

The DMFT results for the $N = 2$ degenerate model are plotted in Fig. 6. DMFT fully confirms the SSMF scenario and the reliability of the SSMF method. The transition boundaries are slightly shifted by DMFT as the SSMF, like SBs, is known to overestimate U_c.

DMFT can also yield a much deeper insight into the physics of the systems through the analysis of dynamical quantities as, e.g., the local self-energies $\Sigma_m(i\omega_n)$ and spectral functions $\rho_m(\omega) = -1/\pi \, Im \, G_m(\omega + i0^+)$, where G_m is the Green's function for band m.
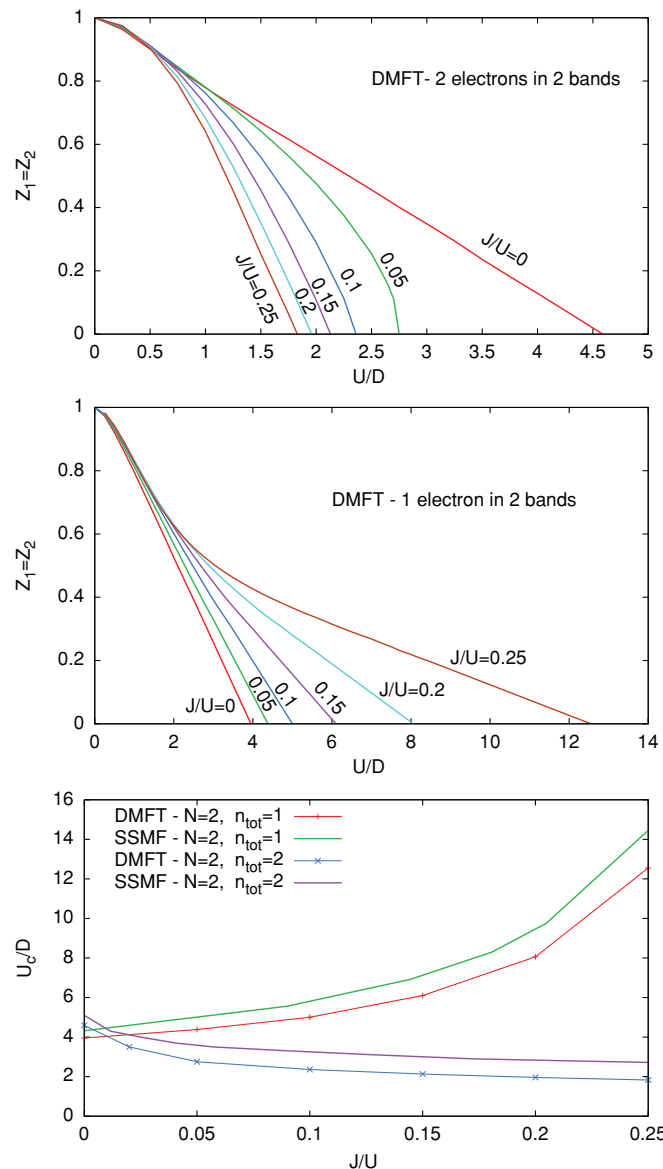

FIG. 6. (Color online) DMFT results for two-band degenerate Hubbard model for the Mott transition with $n = 2$ electrons (upper panel), and $n = 1$ (middle panel) which fully confirm SSMF results. Lower panel: phase diagram comparison between SSMF and DMFT. The slight overestimation of U_c is a known issue of slave-variable mean fields, common, e.g., to SBs.

Figure 7 plots the self-energies at $U/D = 1.75$ as a function of J for the half-filled and quarter filled cases. As expected, J is seen to enhance the self-energy in the half-filled case, thus correlating the system, while it lowers the self-energy in the quarter-filled case and it decorrelates the system.

Figure 7 plots the spectral functions corresponding to the quarter-filled two-band Hubbard model in the metallic phase. The Hubbard bands are very structured, reflecting the multiple energy scales present already in the atomic Hamiltonian.[34] In these bands, the features which are closer to the central peak (that is due to the coherent quasiparticle excitations which disappear at the Mott transition) are the precursors of the lowest atomic excitations. As predicted by the atomic limit arguments these features move closer to the central peak with J.
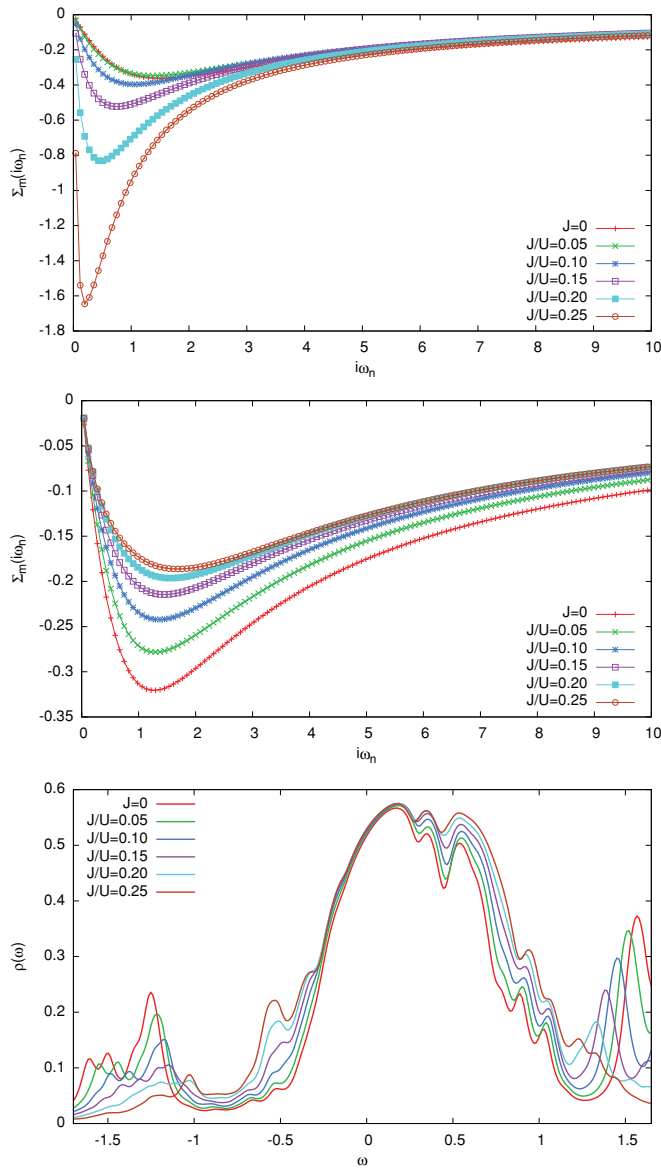
FIG. 7. (Color online) Self-energies of the metallic phase calculated in DMFT for $U/D = 1.75$ as a function of J. Upper panel: two electrons in two bands, the self-energy grows with J. Central panel: one electrons in two bands, the self-energy diminishes with J. Lower panel: spectral functions for the quarter-filled case at low energy. The features of the Hubbard bands closest to the broad low-energy feature (the leftmost and rightmost in the plotted energy window) move closer as J is increased, as predicted by the atomic limit arguments.

We can thus unambiguously draw the conclusion that Hund's coupling works against the Mott transition in all cases but the half-filled one. A *caveat* to this statement is that only the reentrant behavior of U_c (at small J, where the suppression of orbital fluctuations overruns the shifting of the Hubbard bands) can be found for integer fillings close to half, and the effect of strong hybridization and/or crystal-field splitting in the regime $V_{mm'}$ or $\Delta_{mm'} > J$.

Also, moving away from the Mott transition boundary, a subtle interplay of this Mott atomic-like physics with the Kondo screening characterizes the correlated metallic phase. In the two-band Hubbard model these two aspects work together.

In the half-filled case the Kondo temperature is known to be reduced by J,[12,35] while for the quarter-filled case a modest increase of it has been reported,[12] all in line with our results.

For the three-band model the situation is expected to be analogous for both the half-filled and the extremal $n = 1$ ($n = 5$) cases. In the $n = 2$ ($n = 4$) case instead, the relation between the Kondo temperature and the U_c dependence on J is probably less straightforward, in view of the reentrant transition boundary visible in Fig. 5 (also in Ref. 36 a "spin freezing transition" is reported to happen before the Mott transition), and this will be the subject of a future publication.

IV. HUND'S COUPLING AS A BAND DECOUPLER: ORBITAL-SELECTIVE MOTT TRANSITIONS

Thus far we have dealt with only the fully degenerate Hubbard model, where all bands are identical, and we have focused on the influence of the Hund's coupling on the behavior of the system as a whole.

We will now allow for differences between the bands and study systems in the presence of crystal field splitting or differences between the bandwidths. We will in particularly highlight how in these systems the bands can show very different behaviors when J is sizable. For instance, the bands can show a different degree of correlation, and the Mott transition can become selective.

The OSMT has been thoroughly studied in the half-filled Hubbard model with two different bandwidths,[23,26,29,37–41] and it has been shown how Hund's coupling widens the parameter region where the OSMT can be found. However, it has been shown in a recent publication[24] that even systems in which all bands have the same bandwidth can undergo an OSMT when J is beyond a critical value. This has been shown for a three-band model populated by four electrons, in which two bands are degenerate and one is lifted up in energy (inset of Fig. 8). For a large range of crystal field splitting the upper band can open a Mott gap, becoming half-filled, while the other two bands remain metallic.
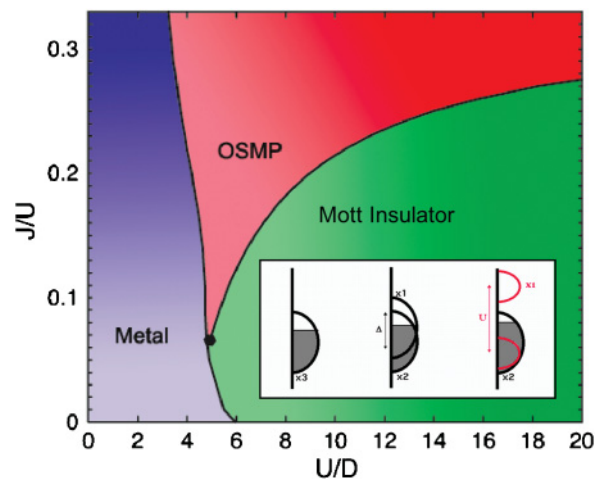

FIG. 8. (Color online) Phase diagram from Ref. 24 for a three-band Hubbard model populated by four electrons, with two degenerate bands and one lifted in energy, as depicted in the inset.

It is worth stressing the important role played by the Hund's coupling. As said, a finite value of J is needed in order to trigger the OSMT. Then further raising J/U widens enormously the selective phase (see Fig. 8), pushing the boundary of the Mott insulating phase at very high U. This being a localization of four electrons in three bands, the quick raise of the U_c necessary for this system to become a Mott insulator is explained by our study of the non-half-filled Mott transition performed in Sec. III.

What is remarkable here is that, while the boundary for the Mott transition of the whole system follows closely the result for the degenerate system (the result for $N = 3n = 2$, equivalent to $n = 4$, of Fig. 1), one band has a completely different behavior and becomes selectively localized at a much smaller critical value of U, which gets further reduced by J.

Even if this effect has been shown not very sensitive to a small splitting of the two degenerate bands, the main effect highlighted in Ref. 24 as possibly responsible for the OSMT behavior is the different degeneracies of the two parts of the system. Albeit having the same bandwidth, the doubly degenerate subsystem has an enhanced kinetic energy that can be seen as an increased effective bandwidth (thus having a different U_c, if it were decoupled from the third band), tracing this OSMT back to the previously studied cases of systems of bands of unequal width.

It is shown here that the main effect causing the OSMT in these system of equal bands is another, namely the suppression of the orbital correlations induced by J.

For this we will study a system far from any degeneracy. We consider a three-band model, Eq. (1), with all equal bandwidths and a trigonal crystal field splitting ($\Delta_{12} = -\Delta_{23}$), at half-filling. Namely one band remains half-filled, one is lifted in energy, and another is symmetrically lowered (inset of Fig. 9).

Results in the SSMF for a sizable Hund's coupling $J/U = 0.25$ are shown in Fig. 9 for different fixed-population imbalances, $n_1 - n_3$. One finds that the half-filled band becomes insulating at a lower critical coupling than the other two, thus opening an orbital-selective Mott phase. The reason for studying the model at fixed $n_1 - n_3$ rather than at fixed Δ is that
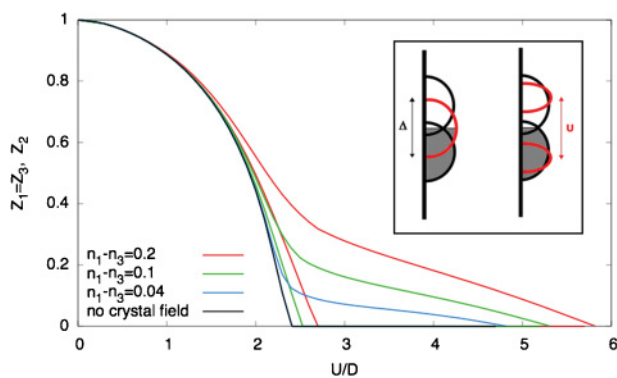

FIG. 9. (Color online) SSMF results for a half-filled three-band Hubbard model with trigonal crystal field splitting. One band remains half-filled, while the other two are shifted symmetrically, as depicted in the inset. The quasiparticle weights $Z_1 = Z_2, Z_3$ are shown here as functions, of the interaction strength U/D for Hund's coupling $J/U = 0.25$ at different fixed population unbalances, $n_1 - n_3$.
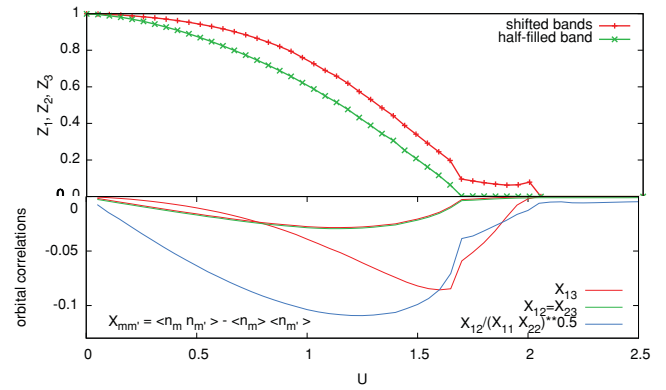

FIG. 10. (Color online) DMFT results for the same model as in the inset of Fig. 9, but fixing the crystal field splitting $\Delta_{12} = -\Delta_{23} = 0.7D$. Upper panel: quasiparticle residues Z_m; lower panel: orbital correlations. A clear suppression of the orbital correlations between the half-filled band and the lifted ones corresponds to the OSMT.

correlations tend to renormalize and strongly reduce the crystal field splitting, so that by keeping the population unbalance fixed the OSMT is enhanced and shown to be possible. We then check the robustness of the OSMT at fixed $\Delta_{12} = 0.7D$ in DMFT and find it in a reduced but still sizable range of correlation strength (Fig. 10).

A complete study of the phase diagram of this model is beyond the scope of this paper; however it was shown that degeneracy is not necessary for an OSMT to happen in a system of all equal bandwidths.

What differentiates the bands here is only the respective individual filling. The system as a whole becomes insulating at a critical U very close to the value $U_c = U_c(N = 3, n = 3, J = 0.25) + \Delta$, where $U_c(N = 3, n = 3, J = 0.25) \simeq 1.15D$, consistent with the atomic picture of the Mott insulator in which the high-spin state is still the ground state and the Mott gap is reduced by the crystal field splitting.

However the half-filled band acts as "decoupled" and the value of U at which it becomes insulating is smaller than U_c for the whole system.

The explanation of this behavior becomes transparent when calculating the orbital correlations,

$$X_{mm'} = \langle (n_m - \langle n_m \rangle)(n_{m'} - \langle n_{m'} \rangle) \rangle$$
$$= \langle n_m n_{m'} \rangle - \langle n_m \rangle \langle n_{m'} \rangle, \qquad (9)$$

in DMFT (lower panel of Fig. 10). It is clear that the OSMT is accompanied by an almost complete suppression of the orbital fluctuations between the half-filled band and the lifted ones. This implies that close to the transition the half-filled band is in practice decoupled and it can become Mott insulating while the others remain metallic. Also the effect of the crystal field will be minor on its Mott gap. Consequently the U_c for this band will be poorly affected by it.

One may think that this suppression of the *inter*orbital fluctuations reflects only the suppression of *intra*orbital fluctuations typical of any Mott transition (owing to the fact that a Mott insulator has a very small double occupancy). This is not the case, here. Indeed Fig. 10 plots the ratio between these quantities $X_{12}/\sqrt{X_{11}X_{22}}$, i.e., the interorbital fluctuations normalized by the standard deviation of the intraorbital ones in
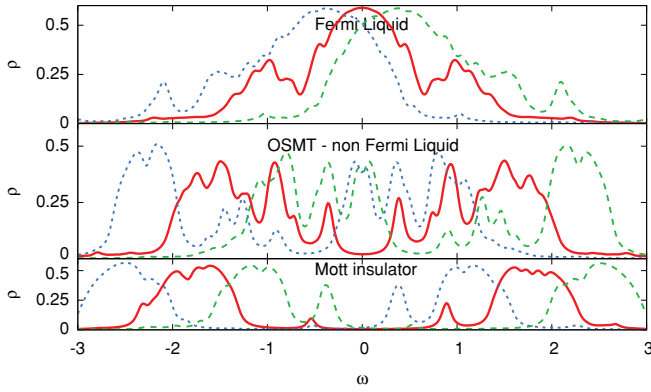
FIG. 11. (Color online) Spectral functions corresponding to the three phases of the data plotted in Fig. 10, for $J = 0.25U$ and $\Delta_{12} = -\Delta_{23} = 0.7D$. Panels from top to bottom: $U/D = 1.0, 1.8, 2.3$. The half-filled band is indicated by the full line, the two shifted bands by blue and green dashed lines. In the top panel all the bands are metallic; in the bottom panel all are Mott insulating. In the middle panel only the half-filled band opens a Mott gap, whereas the two shifted bands are metallic, but the spectral density at the chemical potential violates the pinning condition imposed from the Luttinger theorem, signaling a non-Fermi-liquid state.

each of the involved bands, which drops very fast at the OSMT. This shows that the interorbital fluctuations are suppressed much faster than the intraorbital ones and highlights the role of this suppression driven by J in decoupling the bands and thus inducing the OSMT.

Figure 11 shows the spectral functions corresponding to the three phases (metallic, orbitally selective and Mott insulating) that the model goes through. The orbitally selective Mott phase shows a clear gap in the half-filled band only. It is also characterized by non-Fermi-liquid behavior, here represented by a lowering of the density of states at the Fermi level in the metallic bands.[42]

Thus one can conclude that Hund's coupling acts as a band decoupler, leading, to a first approximation, from a collective to an individual behavior for each band. Then it will be
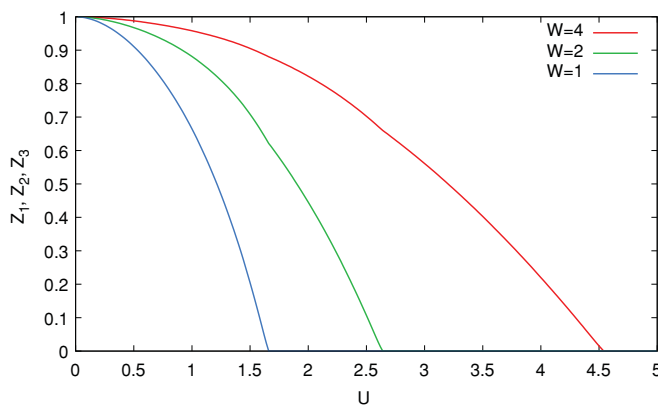

FIG. 12. (Color online) SSMF results for a three-band Hubbard model with bandwidths $W = 4, 2, 1$. All bands are half-filled and $J/U = 0.25$. An almost completely decoupled behavior is induced by J, leading to a cascade of OSMTs whose critical couplings scale roughly with the bandwidths.
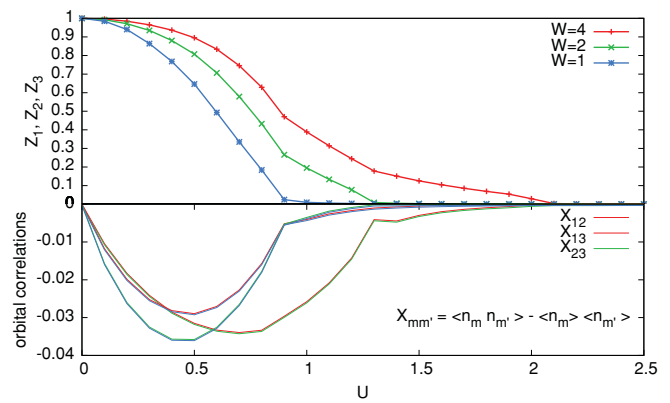

FIG. 13. (Color online) DMFT results for the same model as in Fig. 12. Upper panel: quasiparticle residue for each band; lower panel: orbital correlations, which are suppressed between the localizing band and the itinerant ones, while they remain sizable between the two itinerant bands.

each band's structure and filling that determine the correlated properties.

As another paradigmatic example of such a nearly decoupled behavior a Hubbard model of three half-filled bands with different bandwidths and Hund's coupling $J/U = 0.25$ was studied.

The results are plotted in Fig. 12. As a function of U the three bands undergo a "cascade" of individual Mott transitions at U_c's that scale very roughly with the bare bandwidth of each band, thus testifying to an almost decoupled behavior.

The SSMF results are confirmed by DMFT, as shown in Fig. 13, where the orbital correlations are also plotted, as previously. The same physics is found here, with a strong suppression of the orbital fluctuations between localized and itinerant bands, leading to a decoupled behavior.

V. CONCLUSIONS

This paper analyzes the role of Hund's coupling in tuning the correlation effects in multiorbital materials and is divided into two parts.

The first showed that Hund's coupling in degenerate systems of interacting bands can have two opposite effects, depending on the global filling of the system: In half-filled systems it strongly correlates the system and accordingly lowers the critical interaction strength U_c for the Mott transition. In all other cases the U_c is quickly pushed at very high values by J. This is strictly true when J is strong, and it can be fully understood by analyzing the atomic multiplets. When J is small instead, the suppression of orbital fluctuations (which is maximal at half-filling and decreases quickly, moving away from it) can dominate, enhancing correlations. This enhances the reduction of U_c in half-filled systems and produces a reentrant behavior for fillings close to half—before crossing over to the strong J behavior—while is negligible otherwise.

The second part of this paper addressed non-degenerate systems, where crystal field splittings or bandwidth differences characterize the different bands. In these systems it was shown that the Hund's coupling acts mainly as a band decoupler, through the suppression of the orbital correlations.

At intermediate to strong J, the bands will then have different correlation effects, based on the individual structure or filling. When bands have similar width and structure, the individual proximity to half-filling becomes then a measure of the correlation strength of each band.

In systems where the two effects combine (non-half-filling of the global system and proximity to half-filling of one band or a subset of bands) in the presence of sizable Hund's coupling a strong differentiation can be expected, because correlations in the subsystem will be enhanced by J whereas they can be reduced for the rest of the system. Strongly and weakly correlated electrons can thus be found in the same conduction bands.[43]

Materials of interest with strong Hund's coupling which arguably fall into this category are, e.g., the iron superconductors and $Ca_xSr_{2-x}RuO_4$.[25]

APPENDIX: METHODS

This section details the equations of the two local mean-field methods used in this paper.

In the slave-spin representation, as detailed for example in Ref. [27], we map the original local Hilbert space of the problem onto a larger local Hilbert space that contains as many fermionic degrees of freedom (named $f_{im\sigma}$) as the original plus the same number of auxiliary spin-1/2 quantum variables, one for each $f_{im\sigma}$. We then associate to every state of the original physical space one of the states in this larger space by using the correspondences,

$$\left| n^d_{im\sigma} = 1 \right\rangle \Longleftrightarrow \left| n^f_{im\sigma} = 1, S^z_{im\sigma} = +1/2 \right\rangle, \tag{A1}$$

$$\left| n^d_{im\sigma} = 0 \right\rangle \Longleftrightarrow \left| n^f_{im\sigma} = 0, S^z_{im\sigma} = -1/2 \right\rangle. \tag{A2}$$

In words, when a local orbital and spin state is occupied then the corresponding slave-spin is "up" and if it is empty the slave-spin is "down." With these one-particle local states one can construct the many-particle states as usual.

The enlarged local Hilbert space also contains unphysical states which are excluded by enforcing the local constraint at each site and for each orbital m and spin σ:

$$f^\dagger_{im\sigma} f_{im\sigma} = S^z_{im\sigma} + \tfrac{1}{2}. \tag{A3}$$

In the enlarged Hilbert space the electron number operator is represented by the auxiliary fermion number, i.e., $n^d_{im\sigma} = n^f_{im\sigma}$, but also by the z component of the slave spin $n^d_{im\sigma} = S^z_{im\sigma} + 1/2$, thanks to the constraint. This allows us to rewrite after a little algebra the density-density interaction terms in H_{int} in terms of the spins only:

$$\frac{U'}{2} \sum_i \left(\sum_{m,\sigma} S^z_{im\sigma} \right)^2 + J \sum_{i,m} \left(\sum_\sigma S^z_{im\sigma} \right)^2$$
$$- \frac{J}{2} \sum_{i,\sigma} \left(\sum_m S^z_{im\sigma} \right)^2, \tag{A4}$$

while the nondensity-density terms of the interaction are approximated as[26]

$$-J\sum_{i,m'>m} [S^+_{im\uparrow} S^-_{im\downarrow} S^+_{im'\downarrow} S^-_{im'\uparrow} + S^+_{im\uparrow} S^+_{im\downarrow} S^-_{im'\uparrow} S^-_{im'\downarrow} + h.c.]. \tag{A5}$$

For the nondiagonal hopping operators it can be shown that the most general form allowed in the enlarged Hilbert space is[27]

$$d_{im\sigma} = f_{im\sigma} O_{im\sigma}, \quad d^\dagger_{im\sigma} = f^\dagger_{im\sigma} O^\dagger_{im\sigma}, \tag{A6}$$

in which $O_{im\sigma} = c_{im\sigma} S^+_{im\sigma} + S^-_{im\sigma}$. The choice of the complex number $c_{im\sigma}$ is very important. The arbitrariness of $c_{im\sigma}$ comes from the fact that different operators can have the same effect in the physical subspace of the enlarged Hilbert space, while acting differently on the unphysical states. This difference does not have any effect as long as the constraint is treated exactly. In practice the local constraints are enforced on the average via Lagrange multipliers and the particular choice of $c_{im\sigma}$ matters. It can be tuned in order to obtain the most meaningful mean field, by requiring, e.g., that it yield the correct noninteracting limit (as it happens in SB mean fields[3]).

It can be shown[27] that a suitable choice for a local mean field is such that $c_{im\sigma}$ depends on the average occupation of each orbital in the local state and reads

$$c_{im\sigma} = \frac{1}{\sqrt{n_{im\sigma}(1 - n_{im\sigma})}} - 1. \tag{A7}$$

Finally, in the enlarged Hilbert space the Hamiltonian can be written exactly as

$$H = \sum_{ij,mm'\sigma} t^{mm'}_{ij} O^\dagger_{im\sigma} O_{jm'\sigma} f^\dagger_{im\sigma} f_{jm'\sigma} + H_{\text{int}}[S_{im\sigma}], \tag{A8}$$

subject to constraint (A3).

The mean-field approximation used in this paper consists of three steps: (1) treating the constraints on average, using static Lagrange multipliers $\lambda_{im\sigma}$, (2) decoupling auxiliary fermions and slave-spin degrees of freedom, and finally (3) treating the slave-spin Hamiltonian in a local mean-field approximation. In this paper we consider only paramagnetic phases; hence the mean-fields and the Lagrange multipliers will not depend on the spin σ index.

After these approximations we are left with the mean-field equations:

$$H_f = \sum_{\mathbf{k},m\sigma}(Z_m \varepsilon_{\mathbf{k}m} + \epsilon_m - \lambda_m) f^\dagger_{\mathbf{k}m\sigma} f_{\mathbf{k}m\sigma},$$
$$H_s = \sum_{m\sigma}(h_m O^\dagger_{m\sigma} + h.c.) + \lambda_m \left(S^z_{m\sigma} + \tfrac{1}{2} \right) + H_{\text{int}}[\vec{S}_{m\sigma}],$$
$$Z_m = |\langle O_{m\sigma} \rangle|^2,$$
$$h_m = \langle O_{m\sigma} \rangle \bar{\varepsilon}_m, \tag{A9}$$

where $\varepsilon_{\mathbf{k}m} \equiv \sum_{j \neq i} t_{ij}^{mm} e^{-\mathbf{k} \cdot (\mathbf{i} - \mathbf{j})}$ is the dispersion of band m and $\bar{\epsilon}_m = \frac{1}{N_k} \sum_{\mathbf{k}} \varepsilon_{\mathbf{k}m} \langle f_{\mathbf{k}m\sigma}^{\dagger} f_{\mathbf{k}m\sigma} \rangle$, is the average kinetic energy of each band.

Equations (A9) and average constraint equation (A10), coming from the minimization with respect to the Lagrange multipliers

$$\langle f_{im\sigma}^{\dagger} f_{im\sigma} \rangle = \langle S_{im\sigma}^{z} \rangle + \frac{1}{2}, \qquad (A10)$$

determine self-consistently the effective parameters h_m λ_m, and Z_m and solve the model of Eqs. (1) and (2) in the slave-spin mean-field approximation. Note that the fermionic equation is that of a renormalized noninteracting problem (where Z_m plays the role of the mass renormalization factor and quasiparticle weight), whereas the spin Hamiltonian, even in the mean-field approximation is an interacting problem and has to be diagonalized numerically.

The DMFT[5] is a powerful method for solving a lattice problem in which one assumes the locality of the self-energy. In this case the lattice problem can be mapped exactly onto a quantum impurity problem in the presence of a self-consistency condition. This allows the determination of the local dynamical quantities of the original problem through the solution of this effective impurity problem. The multiorbital model, Eqs. (1) and (2), is thus mapped on the multiorbital impurity problem, the action of which reads (in the imaginary time functional integral formalism)

$$S = -\int_0^{\beta} d\tau \int_0^{\beta} d\tau' \sum_{m\sigma} d_{m\sigma}^{\dagger}(\tau) \mathcal{G}_{m\sigma}^{0}{}^{-1}(\tau - \tau') d_{m\sigma}(\tau') + S_{\text{int}}^{i},$$

$$(A11)$$

where $\mathcal{G}_{m\sigma}^{0}(\tau - \tau')$ represent an amplitude for an electron of spin σ to be destroyed from orbital m at time τ' (jump from the impurity into an effective noninteracting "bath") and being created at time τ (jumping back into the impurity from the effective bath) and S_{int}^{i} is the action term corresponding to the interaction Hamiltonian of Eq. (2) at a given site.

For the present model, where we used semicircular DOSs of half-bandwidth D_m, the self-consistency condition reads

$$\mathcal{G}_{m\sigma}^{0}{}^{-1}(i\omega_n) = i\omega_n - \epsilon_m - \frac{D_m^2}{4} G_{m\sigma}(i\omega_n), \qquad (A12)$$

where $G_{m\sigma}(i\omega_n)$ is the impurity Green's function on the Matsubara axis.

The impurity problem is solved numerically and the calculated Green's function is used to have a new input $\mathcal{G}_{m\sigma}^{0}(i\omega_n)$ through Eq. (A12). The procedure is iterated until convergence is reached. The impurity solver used in this work is the Lanczos exact diagonalization[28] of the Anderson impurity Hamiltonian associated with the action Eq. (A11), where the bath $\mathcal{G}_{m\sigma}^{0}(i\omega_n)$ is represented by a finite number of noninteracting effective sites. In this paper six sites were used for this discretized bath.[44]

---

[1]C. Castellani, C. R. Natoli, and J. Ranninger, Phys. Rev. B **18**, 4945 (1978).

[2]R. Fresard and G. Kotliar, Phys. Rev. B **56**, 12909 (1997).

[3]G. Kotliar and A. E. Ruckenstein, Phys. Rev. Lett. **57**, 1362 (1986).

[4]P. Coleman, Phys. Rev. B **29**, 3035 (1984).

[5]A. Georges, G. Kotliar, W. Krauth, and M. J. Rozenberg, Rev. Mod. Phys. **68**, 13 (1996).

[6]M. Imada, A. Fujimori, and Y. Tokura, Rev. Mod. Phys. **70**, 1039 (1998).

[7]P. Anderson, Science **235**, 1196 (2007).

[8]J. P. Lu, Phys. Rev. B **49**, 5687 (1994).

[9]M. J. Rozenberg, Phys. Rev. B **55**, R4855 (1997).

[10]J. E. Han, M. Jarrell, and D. L. Cox, Phys. Rev. B **58**, R4199 (1998).

[11]A. Koga, Y. Imai, and N. Kawakami, Phys. Rev. B **66**, 165107 (2002).

[12] T. Pruschke and R. Bulla, Eur. Phys. J. B **44**, 217 (2005).

[13]Y. Kamihara, H. Hiramatsu, M. Hirano, R. Kawamura, H. Yanagi, T. Kamiya, and H. Hosono, J. Am. Chem. Soc. **128**, 10012 (2006).

[14]Y. Kamihara, T. Watanabe, M. Hirano, and H. Hosono, J. Am. Chem. Soc. **130**, 3296 (2008).

[15]M. Aichhorn, L. Pourovskii, V. Vildosola, M. Ferrero, O. Parcollet, T. Miyake, S. Georges, and A. Biermann, Phys. Rev. B **80**, 085101 (2009).

[16]M. Aichhorn, S. Biermann, T. Miyake, A. Georges, and M. Imada, Phys. Rev. B **82**, 064504 (2010).

[17]K. Haule, J. Shim, and G. Kotliar, Phys. Rev. Lett. **100**, 226402 (2008).

[18]K. Haule and G. Kotliar, New J. Phys. **11**, 025021 (2009).

[19]J. Wu, P. Phillips, and A. H. Castro Neto, Phys. Rev. Lett. **101**, 126401 (2008).

[20]S.-P. Kou, T. Li, and Z.-Y. Weng, Europhys. Lett. **88**, 17010 (2009).

[21]L. de' Medici, S. Hassan, and M. Capone, J. Supercond. N. Mag. **22**, 535 (2009).

[22]A. Hackl and M. Vojta, New J. Phys. **11**, 055064 (2009).

[23]V. Anisimov, I. Nekrasov, D. Kondakov, T. Rice, and M. Sigrist, Eur. Phys. J. B **25**, 191 (2002).

[24]L. de' Medici, S. R. Hassan, M. Capone, and X. Dai, Phys. Rev. Lett. **102**, 126401 (2009).

[25]J. Mravlje, M. Aichhorn, T. Miyake, K. Haule, G. Kotliar, and A. Georges, Phys. Rev. Lett. **106**, 096401 (2011).

[26]L. de' Medici, A. Georges, and S. Biermann, Phys. Rev. B **72**, 205124 (2005).

[27] S. R. Hassan and L. de' Medici, Phys. Rev. B **81**, 035106 (2010).

[28]M. Caffarel and W. Krauth, Phys. Rev. Lett. **72**, 1545 (1994).

[29]P. Werner and A. J. Millis, Phys. Rev. Lett. **99**, 126405 (2007).

[30]P. Werner, E. Gull, and A. J. Millis, Phys. Rev. B **79**, 115119 (2009).

[31]O. Gunnarsson, E. Koch, and R. M. Martin, Phys. Rev. B **54**, R11026 (1996).

[32]Indeed the DMFT picture of the Mott transition is more articulated and around the actual transition one finds a zone where a metallic and an insulating solutions coexists. Then the U_{c1} where the gap closes and the insulating solution is lost is different from the U_{c2} where the metallic solution disappears because the quasiparticle weight vanishes. This latter quantity is identified with the renormalization factor Z_m calculated in SSMF. Although U_{c1} and U_{c2} may scale differently with the number of bands,[33] it can be safely

assumed that they both increase or they both decrease as a function of physical parameters.

[33] S. Florens, A. Georges, G. Kotliar, and O. Parcollet, Phys. Rev. B **66**, 205102 (2002).

[34] G. Kotliar and H. Kajueter, Phys. Rev. B **54**, 14221R (1996).

[35] A. H. Nevidomskyy and P. Coleman, Phys. Rev. Lett. **103**, 147205 (2009).

[36] P. Werner, E. Gull, M. Troyer, and A. J. Millis, Phys. Rev. Lett. **101**, 166405 (2008).

[37] A. Koga, N. Kawakami, T. M. Rice, and M. Sigrist, Phys. Rev. Lett. **92**, 216402 (2004).

[38] M. Ferrero, F. Becca, M. Fabrizio, and M. Capone, Phys. Rev. B **72**, 205126 (2005).

[39] A. Liebsch, Phys. Rev. Lett. **95**, 116402 (2005).

[40] S. Biermann, L. de' Medici, and A. Georges, Phys. Rev. Lett. **95**, 206401 (2005).

[41] M. Vojta, J. Low Temp. Phys. **161**, 203 (2010).

[42] Actually it has been shown[40] that the fully rotational-invariant H_{int} that we study does not lead to a violation of the Luttinger theorem in the orbitally selective phase at strictly zero temperature. The non-Fermi-liquid behavior is rather signaled by a nonlinear vanishing of the self-energy at low $i\omega_n$. This represents an infinite quasiparticle lifetime at the Fermi energy, which, however, is very sensitive to temperature. Accordingly, when using a finite low-energy resolution, as is done by the discrete exact diagonalization impurity solver (nine total sites) that was used here, this strong temperature dependence shows up as a strong dependence on the low-energy resolution, leading to strong violations of the pinning condition of the zero-energy value of the spectral function of the metallic bands, as is reported in Fig. 11.

[43] It is worth stressing that the models studied in this paper have zero hybridization between the bands. The conclusions of this paper are indeed valid for *weakly hybridized systems*, i.e., they can be extended to nonzero hybridizations with some care. The notion of weakly hybridized system is a basis-independent one. Indeed even if a change of basis can always diagonalize the noninteracting band structure, Wannier orbitals in the new basis are not localized, in general, and the interaction matrix is very non-local then. We call a "weakly hybridized system" one that can be rotated in a basis where both the interaction is local and the hybridization between the orbitals is small. These two conditions cannot be satisfied for all band structures, and are on the contrary a significant constraint, which is material specific.

[44] A comment on the main limitation of DMFT, namely the neglect of nonlocal correlations, is in order. DMFT has been successful in describing the single-band Mott transition,[5] and this description has found many experimental confirmations. However, it is clear that this approach misses a few aspects of the single-band scenario. In single-site DMFT the effective mass diverges at the Mott transition and no precursor effects of the low-temperature ordered phases (such as the antiferromagnet which is the actual ground state in the DMFT treatment of the Hubbard model) in the paramagnetic high-temperature phase are present. Both of these features are artifacts of the local mean field (and the simpler slave variable local mean-fields are no exceptions), and are corrected when more refined approaches, tailored to address nonlocal correlations (such as cluster extensions of these methods, or studies of fluctuations around controlled saddle points representing the local mean-field, when this is possible), are used. None of these aspects is crucial to the present study however, and we have used the (multiorbital) local mean-field approach. The refinements to our general picture that extensions of these multiorbital methods including spatial correlations may yield is surely interesting, and is left for future work.